Parallel Optimization of Flapping Airfoils in a Biplane Configuration for Maximum Thrust

Ismail H. Tuncer[a*] and Mustafa Kaya[a†]

[a]Department of Aerospace Engineering, Middle East Technical University
06531 Ankara, Turkey

Flapping airfoils in a biplane configuration are optimized for a maximum thrust production. A parallel Navier-Stokes solver on overset grids and a gradient based parallel optimization method are employed. The periodic flapping motion of airfoils in a plane configuration is described in a combined pitch and plunge. The pitch and plunge amplitudes and the phase shift between them are optimized for a range of flapping frequencies. It is shown that at low flapping frequencies, flapping airfoils in a biplane configuration produce more thrust than a single flapping airfoil. However, at high flapping frequencies the pitch amplitude tends to go to zero, which promotes an early leading edge vortex formation and limits the thrust production.

Key Words: Parallel optimization, Unsteady flows, Flapping wings, Micro Air Vehicles

1. INTRODUCTION

Based on the performance of small birds and insects, flapping-wing propulsion has received considerable attention in the Micro Air Vehicle (MAV) community in the last decade. The current interest is now in finding the most efficient flapping-wing propulsion technologies to provide the required aerodynamic performance of a MAV flight. Recent experimental and computational studies investigated the propulsive characteristics of single and dual flapping airfoils, and shed some light on the relationship among the produced thrust, the amplitude and frequency of the oscillations, and the flow Reynolds number[1,2]. Navier-Stokes computations have been performed by Tuncer et al.[3,4], Isogai et al.[5] and Anderson et al.[6] to explore the effect of flow separation on thrust and propulsive efficiency of a single flapping airfoil in pitch and plunge oscillations.

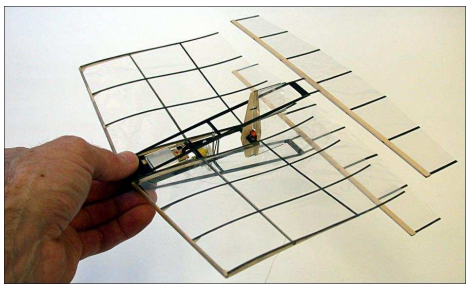

Figure 1: Flapping-wing MAV model (Jones et al.[9])

Recent experimental studies by Jones et al.[7] and Platzer and Jones[8] with two airfoils arranged in a biplane configuration and oscillating in counter-phase showed significant

*Prof., tuncer@ae.metu.edu.tr
†Graduate Research Assistant, mkaya@ae.metu.edu.tr

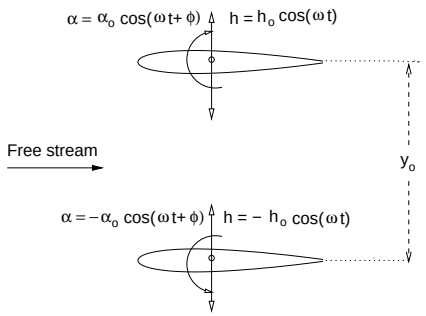

Figure 2. Out-of-phase flapping motion of two airfoils in a biplane configuration

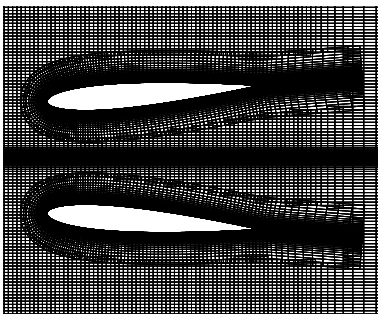

Figure 3. Overset grid system for a biplane configuration

thrust and propulsive benefits in comparison to single flapping foils. Most recently Jones et al.[9] described the development and flight testing of a flapping-wing propelled, radio controlled micro air vehicle (Figure 1).

In an earlier study, Tuncer et al.[10] computed unsteady, viscous flowfields over flapping NACA0012 airfoils in a biplane configuration (Figure 2). In this study, the flapping motion parameters are optimized to maximize thrust using a gradient based parallel optimization method.

2. NUMERICAL METHOD

The unsteady viscous flowfields around flapping airfoils in biplane configuration are computed by solving the Navier-Stokes equations on overset grids. Computations on each subgrid are performed in parallel. PVM message passing library routines are used in the parallel solution algorithm. The computed flowfields are analyzed in terms of aerodynamic loads, instantaneous distribution of flow variables, and unsteady particle traces.

The computational domain is discretized with overset grids. C-type grids around airfoils are overset onto a Cartesian background grid (Figure 3). At the intergrid boundaries formed by the overset grids, the conservative flow variables are interpolated among subgrids in each timestep of the solution [11]. The flapping motions of the airfoils are imposed by moving the airfoils and the computational grids around them over the background grid. The flapping motion of airfoils in plunge, h, and pitch, α, is defined by

$$h = h_o \cos(\omega t) \qquad\qquad \alpha = \alpha_o \cos(\omega t + \phi)$$

where ω is given in terms of reduced frequency, $k = \frac{\omega\, c}{U_\infty}$, c being the chord length. ϕ is the phase shift between plunging and pitching motions.

2.1. Optimization

A gradient based optimization process is employed. The objective function to be maximized is taken as the average thrust coefficient, C_t:

$$C_t = -\frac{1}{T}\int_t^{t+T} C_d \, dt$$

where T is the period of the flapping motion. The gradient of the objective function provides the direction for the steepest ascent to maximize the objective function:

$$\vec{\nabla} O(_{\vec{V}_n}) = \frac{\partial O}{\partial V_1}\vec{v_1} + \frac{\partial O}{\partial V_2}\vec{v_2} + \cdots$$

where V_n denotes the variables of the objective function to be optimized. In this study, The pitch and plunge amplitudes, α_o and h_o, and the phase angle, ϕ are taken as the optimization variables. The objective function is taken as the average thrust produced by the airfoils over a flapping period. The components of the gradient vector is then evaluated numerically by computing the objective function for a perturbation of all the optimization variables one at a time. It should be noted that the evaluation of these vector components requires an unsteady flow solution over a few periods of the flapping motion until a periodic flow behavior is reached.

2.2. Parallel Computation

A coarse parallel algorithm based on domain decomposition is implemented in a master-worker paradigm [12]. The computational grid is decomposed into its subgrids first, and the solution on each subgrid is assigned to a processor. The background grid may also be partitioned to improve the static load balancing. Intergrid boundary conditions are exchanged among subgrid processes. PVM (version 3.4.4) library routines are used for inter-process communication. In the optimization process, unsteady flow solutions with perturbed optimization variables, which are required to determine the gradient vector components of the objective function, are all computed in parallel. Computations are performed in a cluster of computers with dual Pentium-III processors operating on Linux.

3. RESULTS AND DISCUSSION

In the biplane configuration of NACA0012 airfoils flapping in counter-phase, the mean distance between airfoils is set to $y_o = 1.4$ All the flows are computed at $M = 0.1$ and $Re = 1 \cdot 10^4$ assuming laminar flow in accordance with the flying MAV model[9]. The airfoil and background grids are of 141×31 and 135×262 size, respectively. Although the flowfield is symmetric about the mid-plane in the crossflow direction, the full flow domain is discretized to avoid the application of a numerical symmetry condition, and to asses the accuracy of the computations. For parallel computations, the background grid is partitioned into two at the symmetry plane. The computational domain is then decomposed into a total of four subgrids.

Case	k	h_o	α_{oi}	ϕ_i
1a	1.0	0.4	5°	30°
1b	1.0	0.4	5°	60°
2	1.0	$h_{oi} = 0.2$	5°	30°
3	0.5	0.4	5°	30°
4	1.5	0.4	5°	30°
5	2.0	0.4	5°	30°

Table 1: Optimization cases and initial values of the optimization variables

An optimization process starts with arbitrary initial values of the optimization variables. The gradient of the objective function, which is the average thrust coefficient, is next evaluated numerically by perturbing the optimization variables and computing the average thrust coefficient over a few periods of the flapping motion. A small step is then taken along the gradient vector, which increments all the optimization variables. The incremental variation of optimization variables continues until the gradient vector

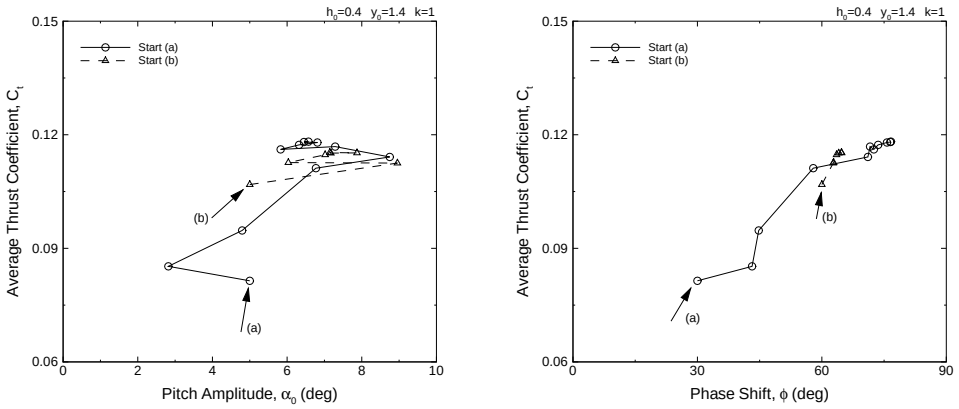

Figure 4. Variation of thrust coefficient along the optimization steps, Case 1a and 1b

vanishes. Table 1 summarizes the optimization cases studied, and the initial values of the optimization variables, V_i. A typical parallel optimization process takes about 10-16 optimization steps. In each step, the gradient vector with as many components as the number of optimization variables is evaluated. Each gradient vector evaluation requires a computation of the unsteady flowfield for about 3-6 periods of the flapping motion. Computation of an optimization case, which may be distributed over 12-16 processors, takes about 120-180 clock hours.

All the optimization results are given in Table 2. Efficiency of the flapping motion given in the table, η, is defined as the ratio of average extracted to input power[9]. The optimization steps for Cases 1a and 1b, for which only the initial conditions differ, are shown in Figure 4. The optimization variables, α_o and ϕ converges to 6.5° and 76.5° respectively for Case 1a, and to 7.9° and 64.7° for Case 1b. In both cases the thrust coefficients are maximized at about $C_t = 0.12$.

Case	h_o	α_o	ϕ	C_t	$\%\eta$
1a	0.4	6.5°	76.5°	0.12	46
1b	0.4	7.9°	64.7°	0.12	45
2	0.4	6.3°	78.4°	0.12	45
3	0.4	0.6°	29.1°	0.01	6
4	0.4	10.5°	92.5°	0.24	48
5	0.4	1.4°	37.6°	0.15	16

Table 2: Optimization results

An instantaneous flow field, which shows the continuity of the flow variables across the overset grid boundaries, is given in Figure 5.

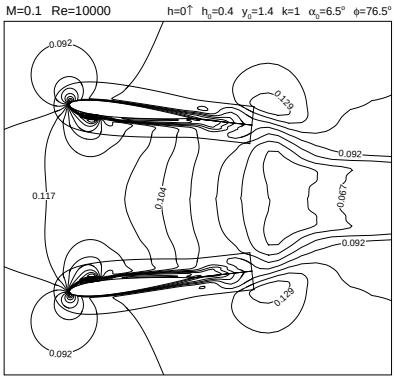

Figure 5: Instantaneous Mach number contours, Case 1a

The unsteady flow field at the optimum condition for Case 1a is given in Figure 6 in terms of particle traces. The particles are released from the vertical lines at the leading edges of the airfoils, and are traced in the flow field with the local flow velocity. As seen in these figures, the unsteady flowfield is highly vortical. The leading edge vortices form on the upper and lower parts of the airfoil during the upstroke and the downstroke, and convect downstream.. It is also noted that the computed flowfield is symmetric about the mid plane. The

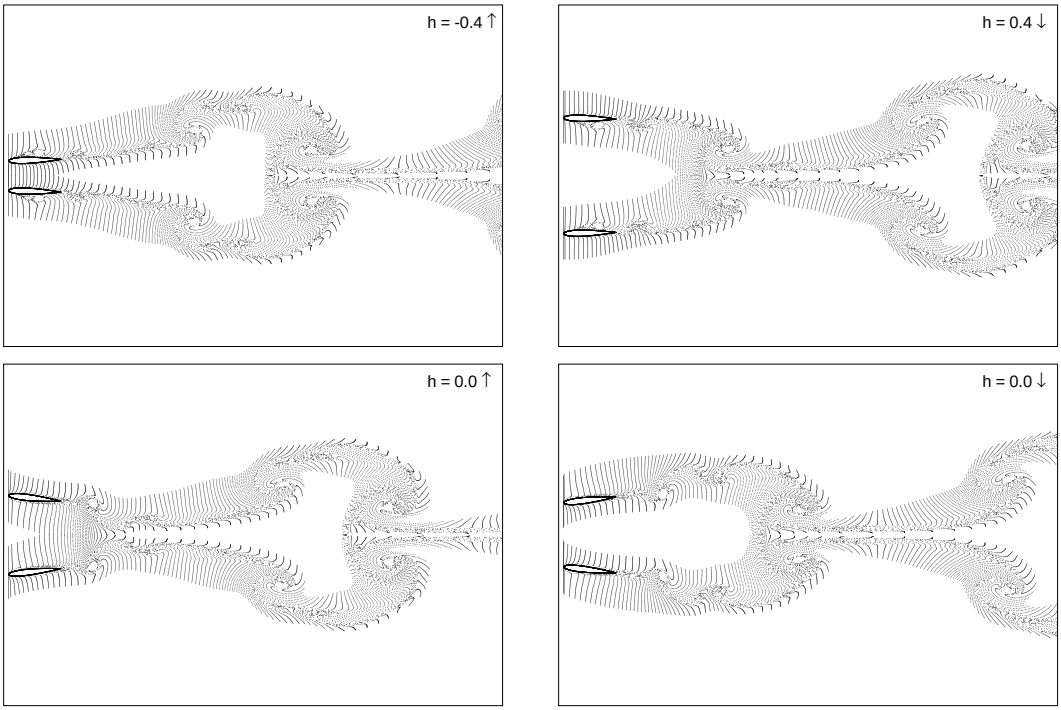

Figure 6. Particle traces along the optimum flapping motion (Case 1a)

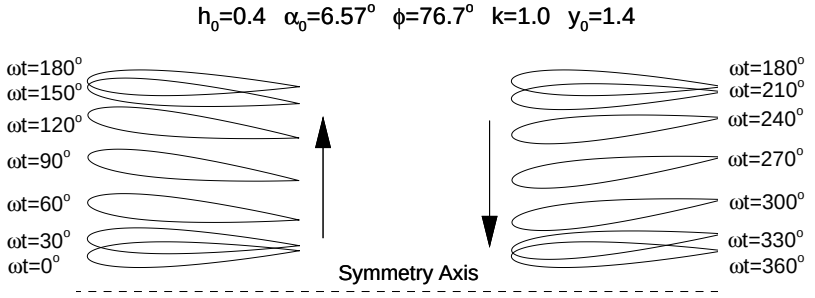

Figure 7. Flapping motion for Case 1a

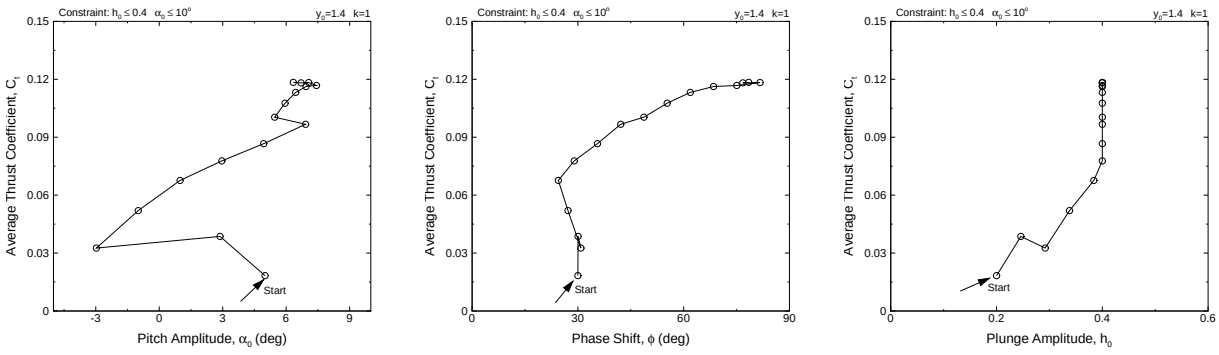

Figure 8. Variation of thrust coefficient along the optimization steps, Case 2

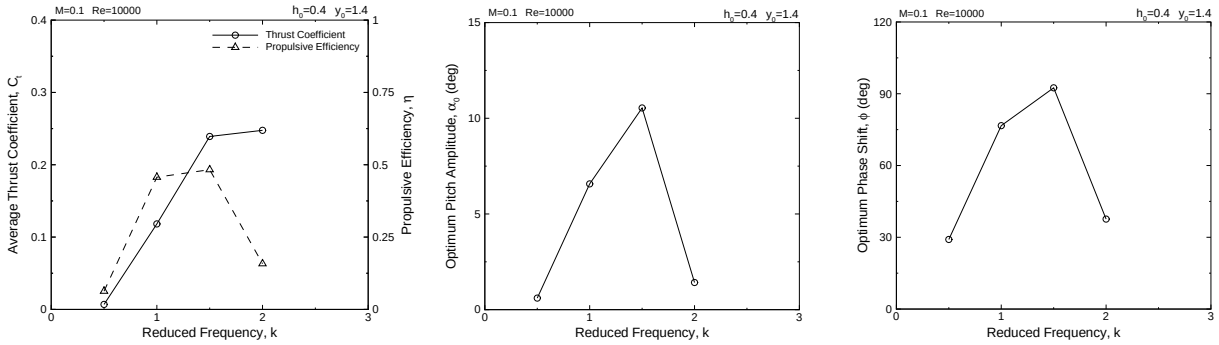

Figure 9. Effect of flapping frequency on the objective function and the optimum values of the optimization variables

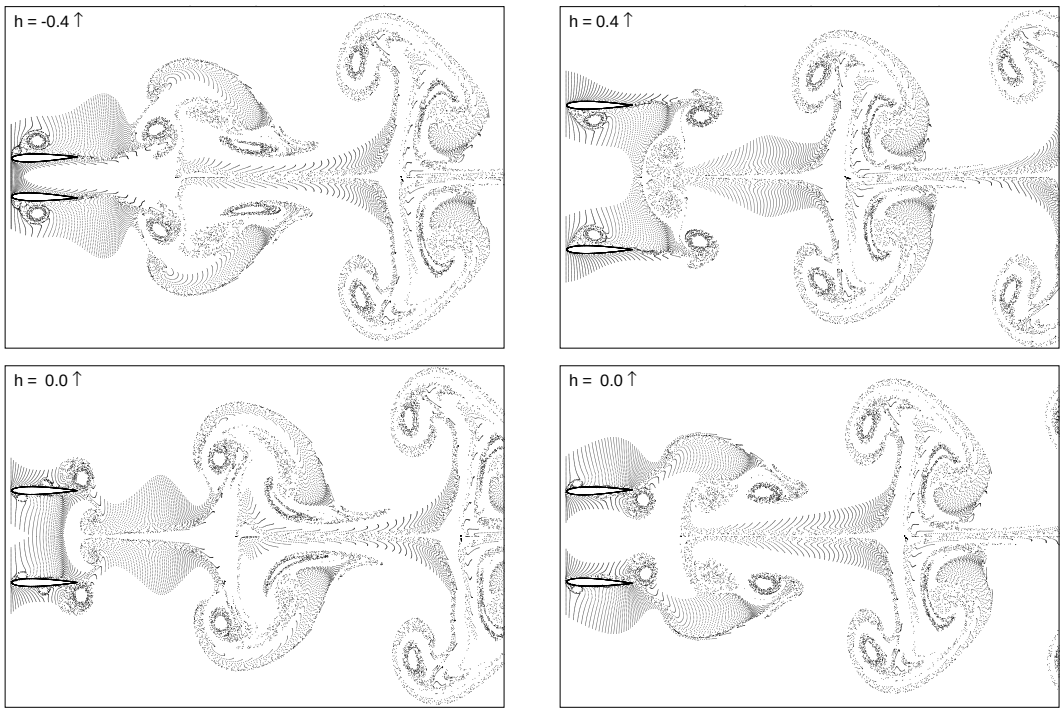

Figure 10. Particle traces along the optimum flapping motion (Case 5)

flapping motion of the upper airfoil is given in Figure 7.

In Case 2, the plunge amplitude, h_o, is included among the optimization variables. However, h_o and α_o are now constrained as $h_o < 0.4$ and $\alpha_o < 10^\circ$ in order to prevent the airfoil grids crossing into each other. The optimization steps are given in Figure 8. As seen, h_o tends to increase as the thrust coefficient increases and, is constrained at $h_o = 0.4$. The optimum condition is in the proximity of the previous cases. Based on the results obtained in Cases 1a, 1b and 2, it is concluded that for $k = 1$ and $h_o = 0.$, the optimization space in which the thrust is maximized forms a ridge along which ϕ tends to decrease as α_o increases around $\alpha_o = 6.5^\circ$ and $\phi = 75^\circ$.

In Cases 3-5, the variation of the maximum thrust and the optimum flapping param-

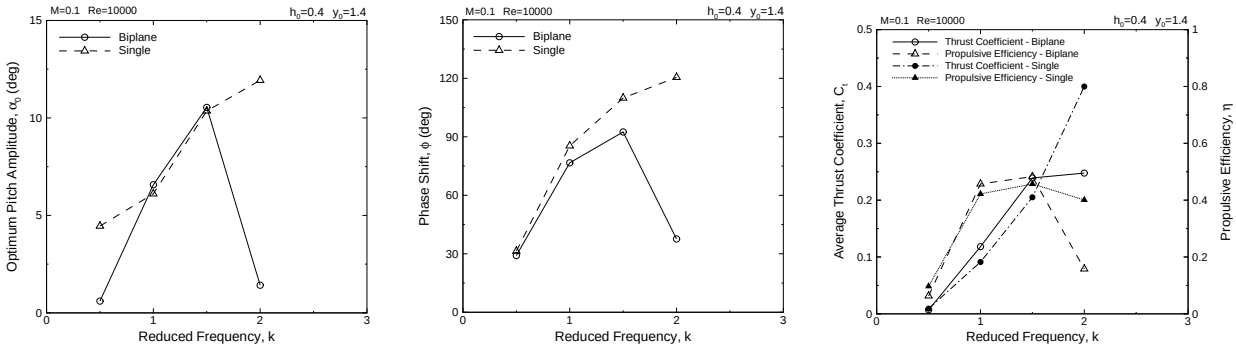

Figure 11. Comparison with a single flapping airfoil.

eters with the flapping frequency are investigated. At $k = 0.5$, flapping airfoils do not produce a significant thrust (Table 2). As the flapping frequency increases the thrust production increases. However, the rate of increase decreases. The variation of the optimum parameters is also given in Figure 9. it is noted that at $k = 2$, the optimum pitch amplitude drops significantly and the airfoils effectively flap in plunge only. The particle traces for this case is given in Figure 10. As a result of the reduced pitch amplitude, the leading edge vortex, which is now stronger, is formed earlier during the opening stroke, and shed into the wake before the airfoils come close together at $h = -0.4$. As a result of reduced pitch amplitude, the blockage between the airfoils seems to be minimized, which incidentally maximizes the thrust.

In Figure 11 the optimum values obtained for the biplane configuration are compared with those for a single flapping airfoil at $h_o = 0.4$. It is seen that up to $k = 1.5$ the maximum thrust produced by the biplane configuration is higher than that of a single airfoil, however, at $k = 2$, the single airfoil produces significantly more thrust than the biplane configuration. It is noted that the single airfoil at the optimum condition for $k = 2$ has a higher pitch amplitude of $\alpha_o = 11.9°$, which delays the leading edge separation, and promotes the thrust production. It appears that in the biplane configuration an early leading edge vortex formation is instead required to prevent a possible vortex blockage between airfoils.

4. CONCLUSIONS

A gradient based optimization is successfully applied to maximize the thrust produced by flapping airfoils in a biplane configuration. At low flapping frequencies, flapping airfoils in a biplane configuration produce more thrust than a single flapping airfoil. At high flapping frequencies, the pitch amplitude tends to go to zero, which promotes early leading edge vortex formations. As opposed to a single flapping airfoil case where thrust production may be increased as the flapping frequency increases, in a biplane configuration thrust production appears to be limited. Current research continues to further investigate the thrust production in a biplane configuration at high frequencies.

REFERENCES

1. Shyy, W., Berg, M. and Lyungvist, D. *Flapping and Flexible Wings for Biological and Micro Air Vehicles* Pergamon Progress in Aerospace Sciences, Vol 35, 1999, p. 455-505.
2. Mueller, T.J. (editor). *Fixed and Flapping Wing Aerodynamics for Micro Air Vehicles*, AIAA Progress in Aeronautics and Astronautics, Vol 195, Reston, VA, 2001.
3. Tuncer, I.H and Platzer, M.F., *Thrust Generation due to Airfoil Flapping,* AIAA Journal, Vol. 34, No. 2, 1995, pp. 324-331.
4. Tuncer, I.H. and Platzer, M.F. *Computational Study Of Flapping Airfoil Aerodynamics*, AIAA Journal of Aircraft, Vol. 35, No.4, 2000, pp. 554-560.
5. Isogai, K., Shinmoto Y., Watanabe, Y., *Effects of Dynamic Stall on Propulsive Efficiency and Thrust of a Flapping Airfoil*, AIAA Journal, Vol. 37, No. 10 pp. 1145-1151, 2000.
6. Anderson, J.M., Streitlien, K., Barrett, D.S. and Triantafyllou, M.S., *Oscillating Foils of High Propulsive Efficiency,* Journal of Fluid Mechanics, Vol. 360, 1998, pp. 41-72.
7. Jones, K.D., Duggan, S.J. and Platzer, M.F., *Flapping-Wing Propulsion for a Micro Air Vehicle,* AIAA Paper No. 2001-0126, 39th AIAA Aerospace Sciences Meeting, Reno, Nevada, Jan., 2001.
8. Platzer, M.F. and Jones, K.D., *The Unsteady Aerodynamics of Flapping-Foil Propellers,* 9th International Symposium on Unsteady Aerodynamics, Aeroacoustics and Aeroelasticity of Turbomachines, Ecole Centrale de Lyon, Lyon, France, September 4-8, 2000.
9. Jones, K.D., Bradshaw, C.J., Papadopoulos, J. and Platzer, M.F. *Improved Performance and Control of Flapping-Wing Propelled Micro Air Vehicles*, AIAA Paper No. 2001-0126, 42nd AIAA Aerospace Sciences Meeting, Reno, Nevada, Jan., 2004.
10. Tuncer, I.H and Kaya, M., *Parallel Computation of Flows Around Flapping Airfoils in Biplane Configuration*, Parallel CFD 2002, Kansai Science City, Japan, May 20-22, 2002
11. Tuncer, I.H, *A 2-D Unsteady Navier-Stokes Solution Method with Moving Overset Grids,* AIAA Journal, Vol. 35, No. 3, March 1997, pp. 471-476.
12. Tuncer, I.H, *Parallel Computation of Multi-Passage Cascade Flows With Overset Grids,* Parallel CFD Workshop, Istanbul, June 16-18, 1999